



ELSEVIER

Tectonophysics 288 (1998) 1–16

TECTONOPHYSICS

Seismic studies around the Kola Superdeep Borehole, Russia

Y.V. Ganchin^{a,*}, S.B. Smithson^a, I.B. Morozov^a, D.K. Smythe^b, V.Z. Garipov^c,
N.A. Karaev^d, Y. Kristofferson^e

^a Department of Geology and Geophysics, University of Wyoming, Laramie, WY 82071-3006, USA

^b Geology and Applied Geology, University of Glasgow, Glasgow G12 8QQ, UK

^c Russian State Committee on Geology, 4-6 B Gruzinskaja, 123242 Moscow, Russia

^d VIRG-‘Rudgeofizika’, 20 Fajansovaja, 193019 St. Petersburg, Russia

^e Institute of Solid Earth Physics, University of Bergen, Allegt. 41, 5007 Bergen, Norway

Abstract

The Kola Superdeep Borehole (SG-3) provided an ideal opportunity to test hypotheses on the origins of crustal reflections and on the presence and seismic expression of fluids in the upper crust. The alternative sources of crustal reflections include compositional changes, shear zones, fluids, and metamorphic facies changes, all of which are represented at the well. Both the 38-km-long CDP section and the borehole VSPs in the range 2.2–6.0 km demonstrate the presence of reflections from dipping compositional layering, shear zones, and fluid-filled zones. Subhorizontal reflectivity zones are interpreted as horizontal fluid-filled fracture-type reservoir rocks. Results suggest the presence of fluids down to a depth of at least 12 km in the upper crust; the presence of these fluids lowering seismic velocity causes estimates of upper crustal composition to be too felsic. © 1998 Elsevier Science B.V. All rights reserved.

Keywords: borehole; CDP; VSP; reflections; Kola

1. Introduction

The geologic interpretation of crustal seismic data is still speculative and raises many questions concerning the nature of crustal reflectors (e.g. Fuchs, 1969; Smithson et al., 1977; Christensen, 1989; Valasek et al., 1989; Kremenetsky, 1990; Pavlenkova, 1991; Mooney and Meissner, 1992; Levander et al., 1994; Rudnick and Fountain, 1995). Mooney and Meissner (1992) suggest a large number of proposed models for the origin of reflections from the deep crust, including: (1) differing physical prop-

erties of rocks; (2) lithologic variations; (3) seismic anisotropy; (4) juxtaposition of different rock types caused by faulting; (5) ductile shear zones; (6) zones containing fluids; (7) ductile flow; (8) molten and partially molten bodies in the crust.

The Kola Superdeep Borehole (SG-3) in the Kola Peninsula, northwest Russia, is one of the few scientific boreholes [e.g. KTB deep drilling project in Germany (Hohrath et al., 1992), Gravberg–Siljan (Juhlin, 1990), Cajon Pass (Rector, 1988)] where hypotheses on the nature of crustal reflectivity can be tested against in situ geological control. The SG-3 borehole has been cored down to the depth of 12.25 km. The comprehensive investigation of its core was carried out together with different kinds of geophys-

* Corresponding author. Fax: +1 (307) 766-6679; E-mail: yuri@uwyo.edu

ical logging experiments in the borehole (Kozlovsky, 1987). Single-fold reflection shooting and deep seismic sounding (DSS) were conducted in the SG-3 borehole region, but until now it has lacked deep-crustal, common-depth-point (CDP) seismic profiling. To fill this major gap in the knowledge of the region, a multinational seismic experiment was performed during winter and spring of 1992. The data acquisition was carried out in cooperation with the Ministry of Geology of the Russian Republic, the Institute of Physics of the Earth of the Academy of Sciences, Moscow, and the Universities of Wyoming, Bergen, Glasgow and Edinburgh. In addition to a ~38-km-long CDP profile, two deep VSPs (up to 6 km deep) and 4 shallow VSPs (0.5 km deep) were acquired during this experiment.

The purpose of this publication is to correlate seismic reflections (present on both VSP and CDP data) with the known geological interfaces along the SG-3 section. This analysis also involves the effect of fluid-filled voids in association with subhorizontal reflectivity detected in VSP and CDP data in the SG-3 vicinity.

2. Main geological and geophysical features of the SG-3 borehole region

The Kola Superdeep Borehole is located in the northeastern part of the Baltic Shield inside the Early Proterozoic Pechenga–Imandra–Varzuga Greenstone Belt, which is surrounded by Late Archean terrains. The main metamorphism, deformation and thrusting in the Belt have occurred ca. 1.95–1.85 Ga (Melezhik and Sturt, 1994), and its evolution is compatible with interpretations in terms of modern plate tectonics (e.g. Berthelsen and Marker, 1986; Melezhik and Sturt, 1994). The early Proterozoic Pechenga structure (Fig. 1), one of the largest zones comprising the Greenstone Belt, can be characterized as a synform consisting of two distinct units: the North and South Zones separated by the Poritash system of faults. The North Zone is an isometric SW dipping (20–60°) half-graben separated into several blocks by a widespread, transverse fault system (Melezhik and Sturt, 1994). The South Zone consists of steeply dipping (40–90°), strongly folded and imbricated rock assemblages.

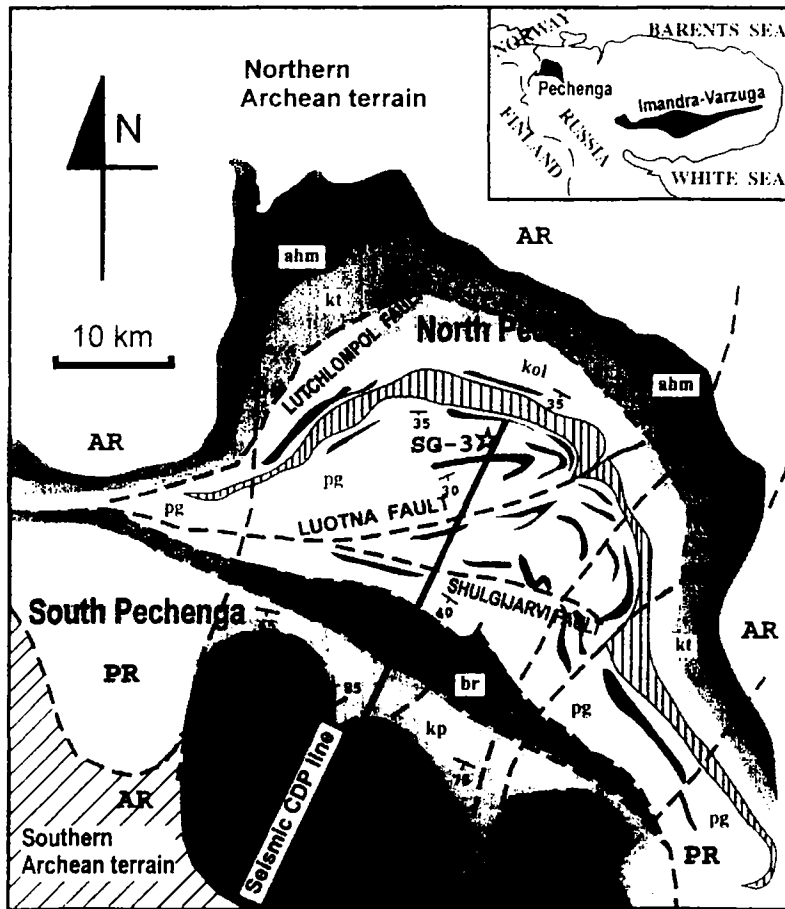
Stratigraphy of the whole Pechenga structure is

characterized by the cyclical build-up of sedimentary–volcanic formations. Each cycle begins with thin sedimentary unit and ends with thick volcanic deposition (Melezhik and Sturt, 1994). Approximately 70% by area, of the structure is occupied by volcanic rocks. The metamorphic grade in the SG-3 section gradually increases with depth from prehnite–pumpellyite to amphibolite facies (Fig. 2), though most commonly it is greenschist in the Proterozoic.

Pillowed and massive tholeiitic basalts and ferropicritic lavas dominate in the upper Proterozoic part of the SG-3 section (0.0–4.5 km deep) and are characterized by P-wave velocity of 6.7–6.8 km/s. Subalkaline basalts with foliated and brecciated texture ($V_p = 6.1–6.3$ km/s) are more widely spread from 4.5 to 6.8 km in the SG-3 section. The most common metasedimentary rocks phyllites, tuffs, and sandstones are characterized by lower sonic P-wave velocities ranging from 5.6 to 6.0 km/s. The rest of the section (6.8–12.2 km) consists mainly of the Late Archean gneiss migmatite rocks ($V_p \sim 6.0$ km/s) hosting abundant amphibolite bodies ($V_p \sim 6.8$ km/s) up to 30 m in thickness. The major shear zone at a depth of 4.5 km where velocity drops from 6.7 to 5.4 km/s is a boundary separating rocks with massive from foliated textures. No definite trend in P-wave velocity variations can be observed in the depth interval 4.5–11.5 km. Below 4.5 km, velocity neither increases nor decreases with depth, though local velocity contrasts reach 1.0 km/s and more. Gneissosity, foliation, and contact surfaces in the whole SG-3 section are commonly parallel to each other and normally dip southwards at angles from 20 to 60°.

Among other gases, helium is the only one that was not affected by technogenic factors during SG-3 gas-logging because it was not present in the drilling mud. In the Proterozoic complex (0–6.8 km) helium accumulations have a local character. Starting from a depth of 7.7 km, the frequency of an anomalous amount of helium increases reaching highest concentrations in between 10.1 and 10.3 km (Fig. 1.66, p. 244 in Kozlovsky, 1987). High gas concentration in the Archean rock complex correlates with the zones of fractured rocks with highly mineralized waters (Fig. 1.77, p. 273 in Kozlovsky, 1987).

Previous seismic studies in the SG-3 region (e.g. Karus et al., 1987; Mints et al., 1987; Kremenetsky,



LEGEND

ARCHEAN ROCKS

a b

 Gneisses, amphibolites, granito-gneisses
 a) northern unit; b) southern unit

EARLY PROTEROZOIC ROCKS

NORTH PECHENGA GROUP

ahm Ahmalahti Formation (polymict conglomerates, sandstones, basalts, basaltic andesites)

kt Kuetsjarvi Formation (red-coloured sandstones, dolostones, alkaline picrites, basalts, andesitic dacites)

kol Kolasjoki Formation (volcanoclastic polymict conglomerates, sandstones, tholeiitic basalts)

pg Pilgjarvi Formation (conglomerates, sandstones, ferropicritic lavas and tuffs, acidic lavas and tuffs)

a b

 a) Ni-Cu bearing 'Productive' Formation, and
 b) acidic lavas and tuffs inside Pilgjarvi Formation

SOUTH PECHENGA GROUP

br Bragino Formation (bimodal picrite-andesite volcanic association, andesitic volcanoclastic conglomerates and sandstones)

kp Kaplja Formation ('black shales', arcose sandstones, cherts, tholeiitic basalts)

INTRUSIVE ROCKS

a b

 a) Orogenic granites; b) subvolcanic andesites

GEOLOGICAL AND OTHER SYMBOLS

a b

 a) Fault; b) strike and dip of bedding

a b

 a) The Kola-92 CDP line location
 b) The Kola Superdeep Borehole location

Fig. 1. Geological sketch map of the Pechenga structure. Modified from Melezhik and Sturt (1994).

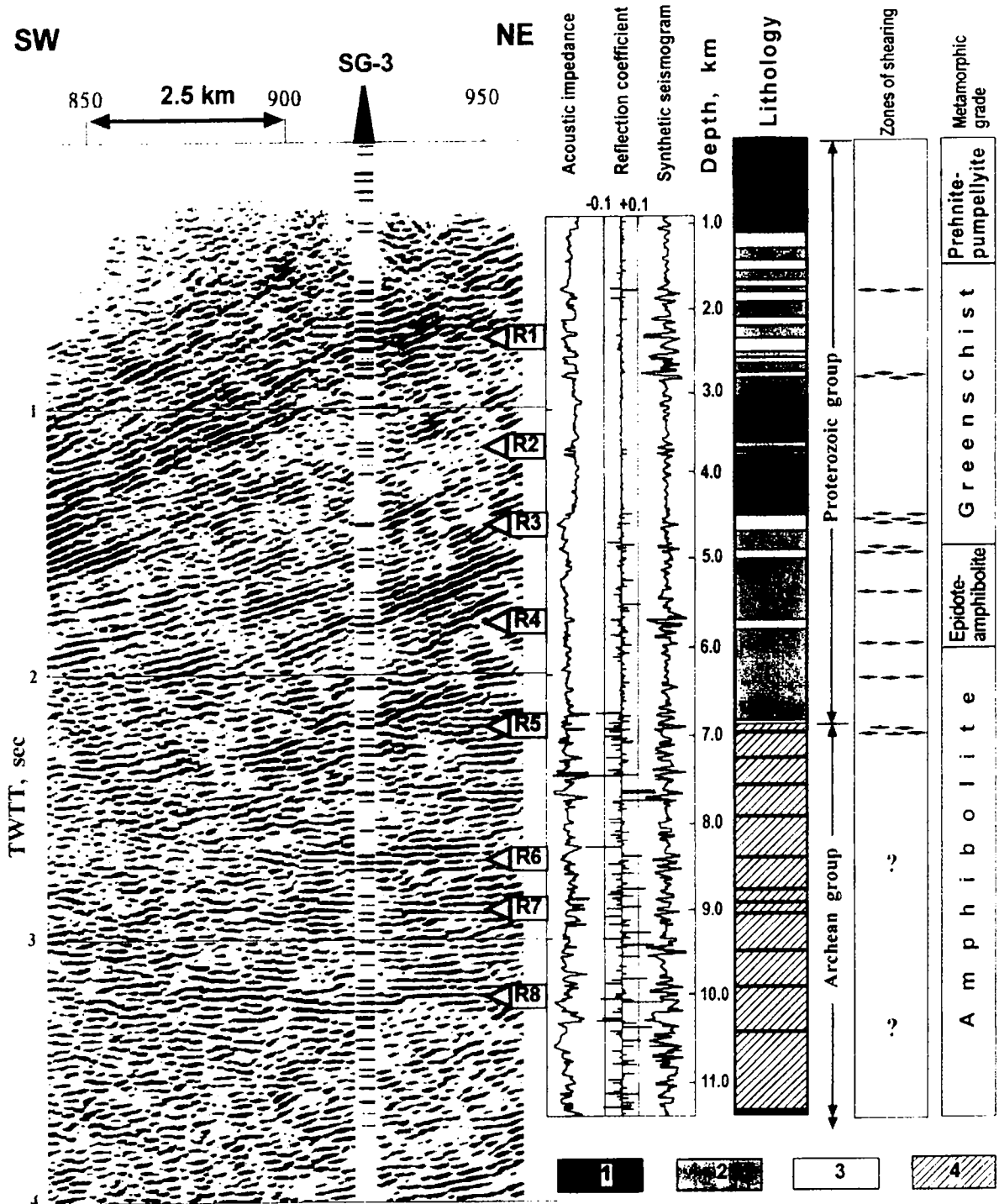


Fig. 2. Northern part of the CDP line (migrated scaled time section) in comparison with the P-wave acoustic log data (acoustic impedance, reflection coefficient, and synthetic seismogram) and geological information from the SG-3 borehole. Synthetic seismogram position on the section corresponds to the borehole location. Lithology explanation: 1 = dominantly massive basalts; 2 = foliated basalts and schists with thin interbeds of metasedimentary rocks; 3 = dominantly metasedimentary rocks; 4 = gneisses with schists and plagiogranites. Horizontal line segments in the Archean denote the thickest amphibolite bodies. R1–R8 denote reflections discussed in the text.

1990; Pavlenkova, 1991; Digranes et al., 1996; Carr et al., 1996) testify to the presence of numerous dipping reflections and subhorizontal reflectors concentrated below 7 km deep (e.g. Pavlenkova, 1991; Mints et al., 1987).

3. 1992 year data acquisition and processing

Approximately 20-fold CDP profiling provided increased signal/noise, lateral resolution and observation density relative to previously conducted seismic investigations in this region. The 38-km-long line was shot from south-west to north-east, along a straight track and ended just north of the borehole. Four seismic vibrators were used as a source, and three recording systems were used for data recording (Table 1). Besides the major CDP line, two deep VSPs were recorded in the Kola Superdeep Borehole from a depth of 2.2 to 6.0 km at 25-m intervals. The source offset was 0.2 km south of the well for VSP-1 and 2.08 km north of the well for VSP-2.

The CDP line was processed to 15 s using an in-

Table 1
The Kola-92 data acquisition parameters

Parameter	Description
<i>Recording</i>	
Instrument	MDS-10 recording system
Number of channels	96
Coverage	20-fold nominal
Recording time	40 s
Correlated record length	20 s
Sample rate	CDP, 4 ms; VSP, 2 ms
<i>Source</i>	
Source type	Falling vibrators
Peak force	27,000 pounds
Number of vibrators	3–4
Number of sweeps	8
Upsweep frequencies	CDP, 10–60 Hz; VSP, 15–90 Hz
Sweep length	20 s
Source interval	100 m nominal
Configuration	Off-end
<i>Receiver</i>	
Geophone type	10 Hz Geosource MD81 (vertical) 10 Hz I.R.S. (horizontal)
Receiver interval	50 m
Geophone array	10 phones spaced 2.5 m
Number of components	3 (1 vertical and 2 horizontal)
Nominal offset variations	1000–5450 m

Table 2

The Kola-92 CDP processing parameters

Parameter	Description
<i>Pre-CDP processing</i>	
Correlation	Synthetic 10–60 Hz upsweep
Interactive editing	Trace killing
Noise-adaptive filtering	Stationary 'machinery' noise (50 Hz and its harmonics and 18 Hz from pumps at the well)
Vertical trace stacking	Diversity stack
<i>CDP pre-stack processing flow (all ProMAX tools)</i>	
2-D line geometry	
Refraction statics	
First-break picks	Interactive
Refraction statics	Interactive
Datum	320 m
Spectral balancing	Pass band 10–60 Hz
KLT noise canceler	Noise-adaptive filter based on the eigen-decomposition of the data covariance matrix
Velocity analysis	Repeated three times
SORT to common offset domain	
NMO	
DMO	
Inverse NMO	
Velocity analysis	Semblance and CVS
SORT to CDP domain	
NMO	Final velocities
CDP stack	
<i>Post-stack processing (all ProMAX tools)</i>	
FX-deconvolution	Random noise elimination
FK and finite-difference	
Migration	

teractive and iterative processing sequence (Table 2). The 1992 Kola VSP data processing was reported by Carr et al. (1996). Two additional processing steps were added in the present study: (1) interval velocities were obtained using least-squares inversion of travel times (Stewart, 1984); (2) deep reflections on multicomponent VSP records were analyzed using 2-D ray-tracing for dipping interfaces.

4. Seismic wavefield description

4.1. The seismic section along the whole CDP line

The seismic section along the whole CDP line shows numerous reflections, mostly dipping SW (Fig. 3a). The section can be subdivided into three

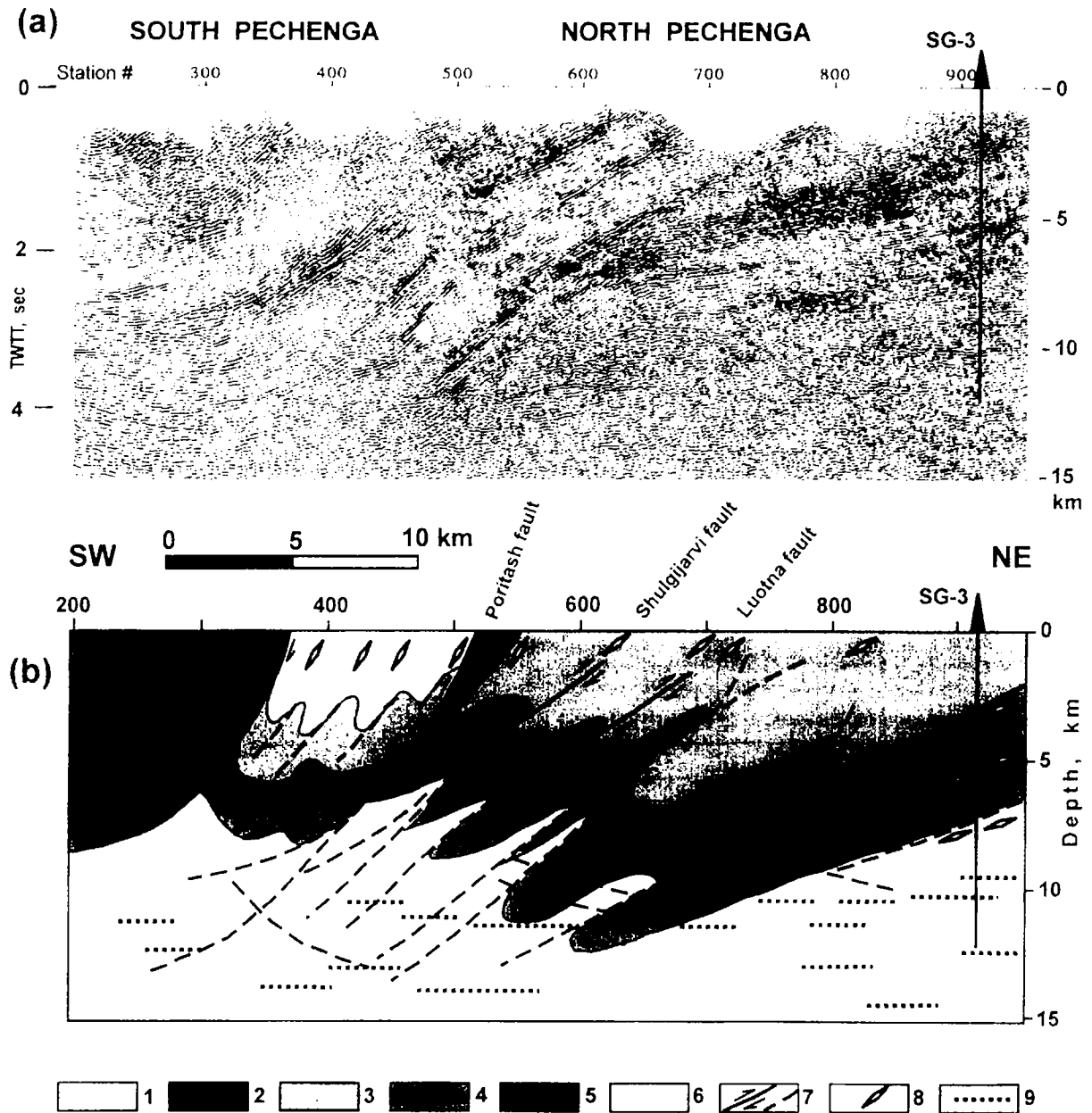


Fig. 3. Seismic section along the Kola CDP line (a). Post-stack finite difference migration. No vertical exaggeration. Interpretative cartoon (b) showing major fault zones and lithological units. 1–2 = South Pechenga Group, 1 = metabasalts and metasediments, 2 = metaandesites; 3–4 = North Pechenga Group, 3 = metabasalts and metasediments of Pilgjarvi Formation, 4 = metabasalts and metasediments of Kolasjoki, Kuetsjarvi and Akhmalahiti Formations; 5 = Early Proterozoic rheomorphic granitoids; 6 = Archean rocks; 7 = faults with arrows indicating relative movement, dashed where inferred; 8 = zones of intense schistosity, foliation and mylonitization showing approximate dip direction; 9 = zones in the crust corresponding to subhorizontal seismic reflectivity.

laterally distinguishable parts: the northern part with gradually flattening south dipping reflectors (from 30 to 10°); the central part, which is characterized by

monoclinal (~30° SW) dip of reflectors which cut off the northern part at about surface station location 800; and the southern part which interferes with the

central part in the vicinity of station number 500. Reflections with the maximum SW dip ($50\text{--}60^\circ$) can be found south of station 500.

The most coherent and continuous SW dipping reflections on the section are interpreted as the fault zones mapped on the surface (Fig. 3b). The Lutona fault (station 740) manifests transition from relatively undisturbed layering in the northern part to strongly faulted and folded rocks occurring in the central part of the section. The Poritash fault zone (station 520) is geologically characterized by a system of closely spaced imbricate thrust faults along which the South Pechenga sequence was thrust onto the North Pechenga units. The southernmost part of the profile crosses a region of granitoid intrusion which may be allochthonous. The corresponding reflections from tectonized contact between granitoids and surrounding rocks can be found south of station 400.

Numerous subhorizontal reflections with different degrees of coherency can be observed throughout the whole section (Fig. 3). Several mechanisms can be suggested for their generation: (1) subhorizontal dikes; (2) subhorizontal faults, juxtaposing different rock types; (3) fluid-filled fracture zones; (4) side-slip. We shall discuss below those of subhorizontal reflections, which appear in the vicinity of the SG-3 borehole.

4.2. Kola 1992 VSP wavefield patterns

The first arrivals observed in the Kola VSPs correspond to an incident P-wave of complicated shape due to reverberations and mode conversions on numerous interfaces (Figs. 4 and 5). Next arrives an incident shear wave with velocity about 1.72 times slower than the direct P-wave. It also comprises several trains of reverberations and mode conversions.

Reflected waves have shorter continuity and less amplitude than the direct arrivals, but still can be easily recognized like those marked A, B, and C in Figs. 4 and 5. As noted by Karus et al. (1987), short coherent line-ups of the up-coming waves and the complex structure of the geological medium do not permit unambiguous determination of the reflection wave type. But in some cases, due to available geological and geophysical information, unambiguous determination of wave type is possible. Several representative continuous reflections were

picked for ray-tracing analysis in the time range 0.5–4.5 s on the vertical (Z) and two horizontal (X and Y) components of VSP-1 and VSP-2 (Figs. 4 and 5). Some possible solutions for the picked reflections are presented in Tables 3 and 4 after comparison of calculated travel times with the observed ones.

The major conclusions from analysis of the VSP reflected wavefield are: (1) SS and PS reflections dominate over PP- and SP-type; (2) moderately dipping ($15\text{--}40^\circ$) interfaces can be found mostly in the Proterozoic part of the section (up to 6.8 km deep); and (3) subhorizontal reflections dominate in the Archean part (at least for the northernmost VSP-2). Points 2 and 3 repeat previously reported results (e.g. Carr et al., 1996; Mints et al., 1987; Pavlenkova, 1991), but point 1 needs to be explained.

The direct shear wave from VSP-2 was subjected to polarization analysis by Digranes et al. (1996). They have observed two clear orthogonal polarizations in the interval from 4.4 to 6.0 km. The theoretical polarizations were calculated for several models. Digranes et al. (1996) report that only the model containing aligned, vertical cracks can explain their observations.

Gibson and Ben-Menahem (1991) presented the P, SV and SH radiation patterns for two cases: (1) isotropic with randomly oriented fractures; (2) anisotropic with aligned cracks. They have established some distinct differences in the scattered displacement fields. In particular, considering the incident P-wave, the backscattered P-wave field for aligned fractures is less than twice that for the isotropic obstacle (figs. 5 and 6 in Gibson and Ben-Menahem, 1991). However, the shapes of the radiation patterns for SV incidence are the same. The radiation patterns (Gibson and Ben-Menahem, 1991) in case of the anisotropic volume explain relatively strong PS and SS reflections on the Kola VSPs (Figs. 4 and 5).

4.3. Wave patterns on the CDP section in the SG-3 vicinity

The seismic wavefield in the vicinity of the SG-3 borehole (Fig. 2) can be subdivided into two parts, the SW dipping reflectors in the time range 0–2.2 s and nearly horizontal reflectors below 2.2 s. The dominant dip of reflectors cross-cutting the SG-3

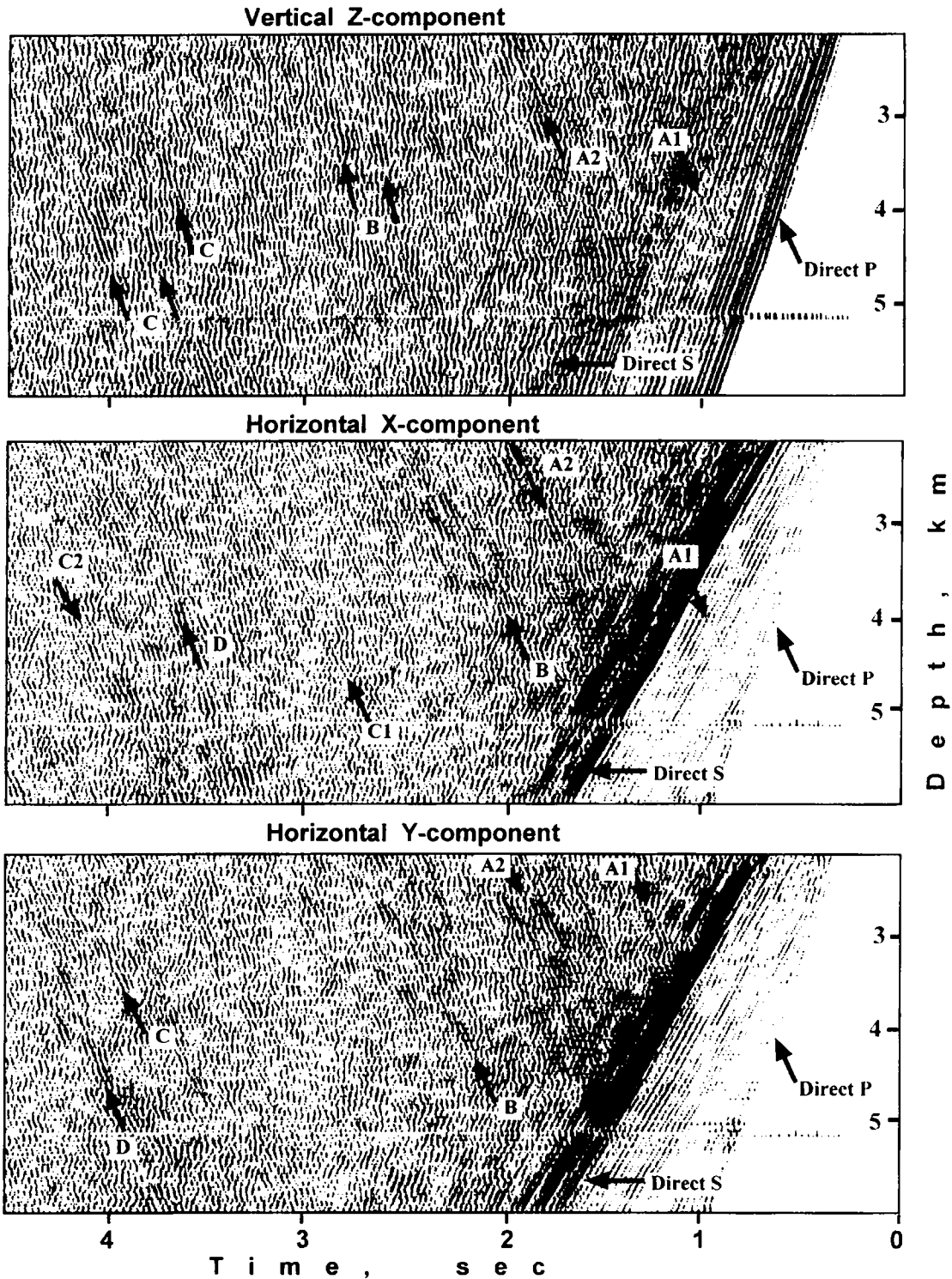


Fig. 4. VSP-1 three-component display. Source, 0.2 km south from the borehole; band-pass filter, 22-58 Hz; AGC, 1000 ms. Arrows indicate reflections discussed in the text and interpreted in Table 3.

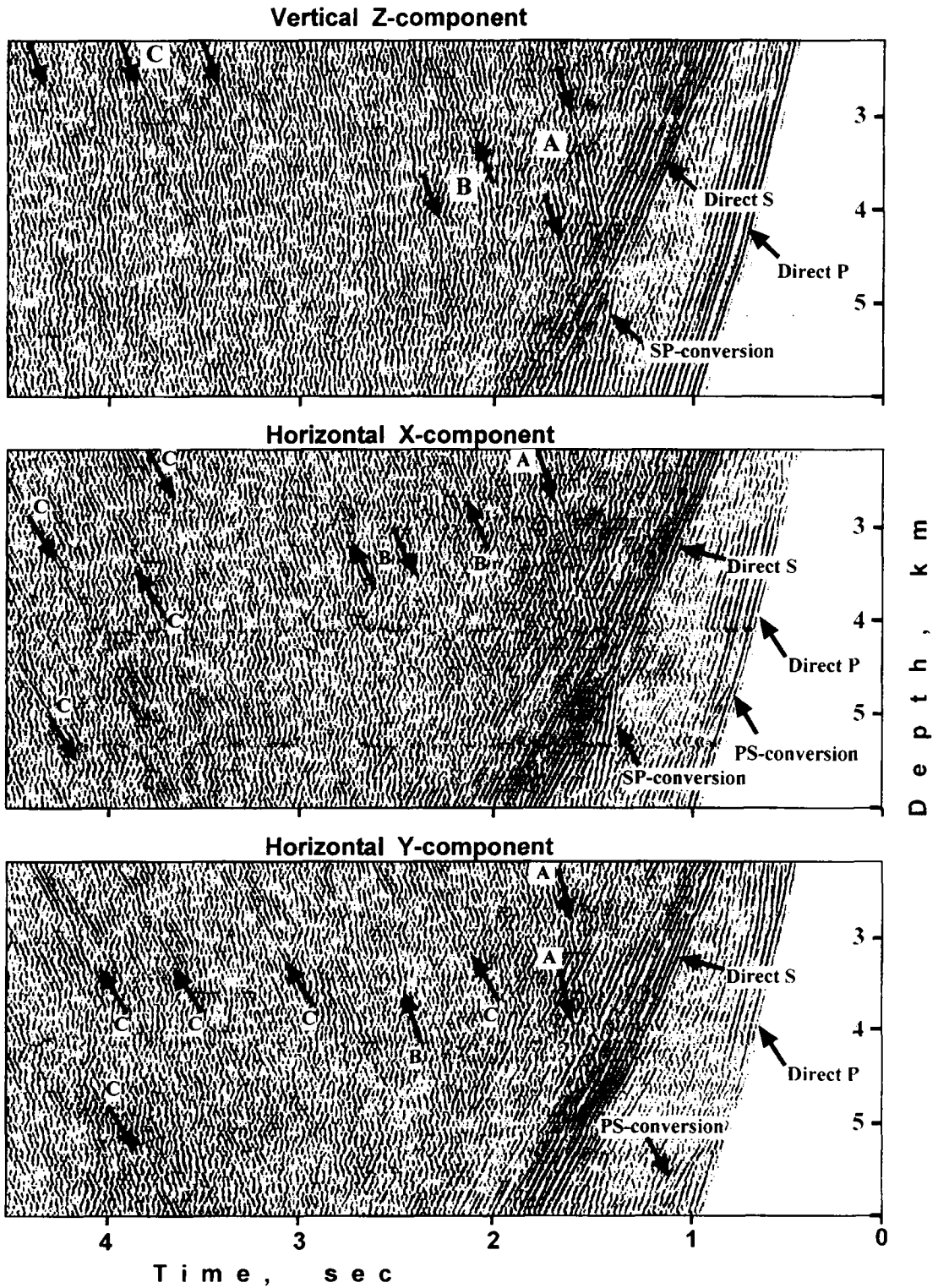


Fig. 5. VSP-2 three-component display. Source, 2.08 km north from the borehole; band-pass filter, 22–58 Hz. Gain corrected for geometrical spreading. Arrows indicate reflections discussed in the text and interpreted in Table 4.

Table 3
Ray-tracing results for reflectors from VSP-1 seismic wavefield^a

Component	Reflector	Apparent velocity (km/s)	Reflected wave type	Reflectors		Angle of	
				Dip (degrees)	Depth (km)	Incidence (degrees)	Approach (degrees)
Z	A1	4,500	PS	25	4.9	5–20	28–37
	A2	4,500	SS	25	4.9	4–20	30–45
	B	8,200	PP	15	~11.	3–6	3–6
			SP	30	~8.0	5–20	35–55
			SS	35	8.0–11.0	5–15	38–55
C	5,100	SS	35				
X	A1	4,500	PS	25	4.9	5–20	28–37
	A2	4,500	SS	25	4.9	4–20	30–45
	B	4,500	SS	25	~6.0	4–18	30–40
	C1	3,700	SS	0	~7.0	0–2	0–2
	C2	3,700	SS	0	~9.0	0–2	0–2
	D	5,300	SS	35	~9.0	5–15	38–55
Y	A1	4,500	PS	25	4.9	5–20	28–37
	A2	4,500	SS	25	4.9	4–20	30–45
	B	4,500	SS	25	~6.0	4–18	30–40
	C	3,800	SS	0	~8.5	0–2	0–2
	D	5,200	SS	35	~11.0	4–14	36–52

^a Source offset 0.2 km south of the borehole.

axis is 25–30° (above 2.2 s). Reflections R1–R5 (Fig. 2) are associated with acoustic contrasts inside the Proterozoic Pechenga complex. A group of

coherent reflections R1 inside the 'Productive' Formation (1.1–2.8 km deep) correspond to contacts of metasedimentary layers with ultramafic intrusions.

Table 4
Ray-tracing results for reflectors from VSP-2 seismic wavefield^a

Component	Reflector	Apparent velocity (km/s)	Reflected wave type	Reflectors		Angle of	
				Dip (degrees)	Depth (km)	Incidence (degrees)	Approach (degrees)
Z	A	8,500	SS	25	4.5, 5.2	25–45	50–70
			PP	0	8.0, 9.0	8–10	6–12
	B	5,800	SS	30	5.5, 6.5	30–40	60–70
			PS	40	8.0, 9.0	20–40	50–70
			SP	0	7.0–11.0	6–8	4–10
	C	6,500	SS	35	8.0–12.0	12–25	45–60
			PP	0	12.0–14.0	6–8	4–8
X	A	7,500	SS	20	4.5	20–40	40–60
			SS	25	5.5–7.0	18–42	50–70
	B	4,600	PS	30	6.0–10.0	15–35	55–75
			PS	0	9.0–12.0	5–7	4–8
			SS	0	7.0–10.0	6–8	4–8
Y	A	9,500	SS	30	4.7, 5.2	30–50	60–80
			PP	35	~11.0	12–25	45–60
	B	11,000	SP	35	~8.5	15–30	40–50
			PS	0	6.0–11.0	5–8	4–8
			SS	0	6.0–11.0	5–8	4–8

^a Source offset 2.08 km north of the borehole.

These boundaries are characterized by the largest velocity contrasts (more than 1.0 km/s), and the corresponding reflections are among the strongest in the CDP section. The reflectivity character of the rocks constituting the 'Productive' strata is enhanced by several shear zones associated mostly with metasedimentary layers. Several relatively thin (10–20 m) horizons of sedimentary–tuffogenic rocks ($V_p = 5.7$ – 6.0 km/s) intercalated with sheets of massive and globular lavas ($V_p = 6.7$ km/s) at a depth of 3.65–3.85 km produce visible coherent reflections R2. Reflection R3 manifests a transition in the SG-3 section between rocks with massive texture and foliated ones (4.5 km deep). This depth also corresponds to the top of the major Lutchlompol Fault Zone (LFZ, 4.5–4.7 km deep), where P-wave velocity drops by more than 20%. In spite of such velocity contrast, the reflection coefficients do not exceed 0.08 in the LFZ (Fig. 2) because of the gradual character of this zone.

The multicyclic reflection R4 can be associated with a metasedimentary layers (meta- limestones, sandstones, and carbonate schists in the depth range 5.65– 5.75 km) inside foliated basalts and plagioclase schists. Though the velocity contrast in this interval is relatively small (5% and less), we observed increased amplitudes on both the synthetic seismogram and the CDP section (Fig. 2). This results from laminated geometry of reflectors. The laminated configuration below the LFZ (4.5 km) is produced not only by sedimentary layers alternated with basalts, but also by zones with strong cataclastic fabrics within layers of unmylonitized rocks. Two important characteristics of mylonitic rocks – preferred orientation of minerals and retrograde mineralogy (Fountain et al., 1984) – suggest that velocities for waves traveling normal to mylonitic layering can be substantially reduced with respect to unmylonitized rocks. Preferred orientation of minerals, particularly biotite or other phyllosilicates, can be expected to cause anisotropy below the LFZ (reflections R3–R5 in Fig. 2).

The Proterozoic–Archean (Pr–Ar) contact (6.84 km deep in the SG-3 section, reflection R5 in the seismic section) juxtaposes Proterozoic diabase schists and Archean gneisses. The P-wave velocity drops to 5.7 km/s in the corresponding depth interval. Only in situ increased fracturing or anisotropy

can explain such velocity drop. Reflection R5, corresponding to the Pr–Ar contact is, most likely, caused by a fault zone dipping in the same general direction as the whole Pechenga structure. This fault zone changes physical characteristics of the rocks comprising it, making them less competent and more fractured that decreases acoustic properties. Compared to the dipping reflection R5, the reflection R6 is nearly horizontal, as well as the deeper ones R7 and R8 (Fig. 2). The possible nature of these sub-horizontal reflections will be discussed below, after a correlation of reflections found on the CDP section with those from the near-offset VSP-1.

4.4. Correlation of CDP and VSP reflectivity patterns

The correlation of CDP and VSP reflectivity patterns is displayed in Fig. 6. Due to predominantly dipping interfaces in the upper Proterozoic part of the SG-3 section, it is unlikely to calibrate the CDP section by means of conventional corridor stack based on a simple flattening of first-break times (Fig. 6a). Instead, better results are obtained by a corridor stack performed after flattening of reflections by precalculated dip moveout corrections (Fig. 6b). Such DMO corrections were obtained by the means of ray-tracing for the known velocity model (based on integrated AI data and inversion of VSP first arrivals) and variable dip angles of interfaces. A dip angle of 25° was found to produce the best P-wave flattening results for VSPs at least in the LFZ vicinity. This value is in general agreement with geological observations and with the results of VSP ray-tracing for the SS reflections from the LFZ (Tables 3 and 4). The resulting corridor stack (Fig. 6b) positions properly the reflector R1 and makes the reflector R2 much more pronounced compared to conventional stack (Fig. 6a). Reflections R3 and R5 corresponding to LFZ and Pr–Ar contact, respectively, as well as the multicyclic reflections between them are in accordance with surface CMP reflections (Fig. 6b). There is a long train of reflections below the Pr–Ar contact which is difficult to correlate with the CDP data. To understand better the reflectivity patterns on both VSP and CDP data, another corridor stack using DMO corrections for SS reflections was performed. After the stacking, the resultant trace was rescaled

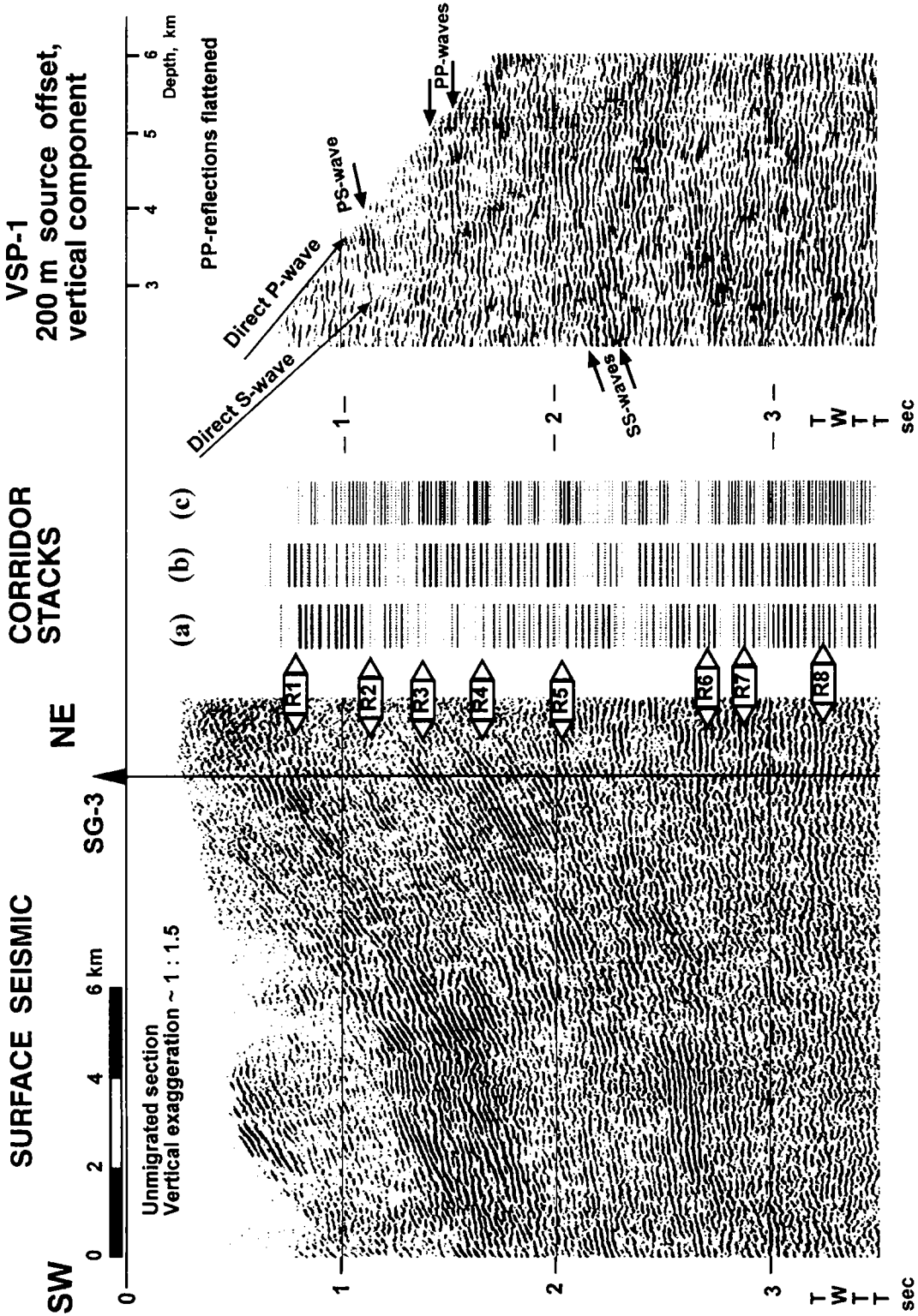


Fig. 6. Correlation of the upgoing wavefield from the VSP with the surface seismics. The corridor stacks are produced by summing VSPs after flattening (a) by the direct P-wave arrivals, (b) by 25° dip moveout corrections for PP-reflected wave, and (c) by 25° dip moveout corrections for SS-reflected wave (rescaled in time to PP-wave arrivals). The single traces from corridor stacks are repeated for visual effect. VSP-1 is plotted after corrections for geometrical spreading, FK-filtering (downgoing wavefield rejected), and flattening by 25° dip moveout corrections for the PP-reflected waves.

($T_s/T_p = V_p/V_s = 1.72$) and plotted (Fig. 6c). In such a stack, the reflections R3–R6 became much more pronounced than on PP wave corridor stack. This observation is in accordance with the radiation patterns by Gibson and Ben-Menahem (1991) for an anisotropic scattering volume. The deeper reflections on an SS wave stack (Fig. 6c) are concentrated around 3 s (9.5 km deep), and according to our interpretation (Tables 3 and 4) they originate from horizontal interfaces.

5. Discussion: causes of velocity variations in the crust sampled by the Kola Well

One way to correlate lithologic cross-section of a crustal segment with the corresponding data derived from sonic logs and VSPs is direct measurement of elastic wave velocities in core samples at high confining pressures when most of microcracks are closed. Vernik et al. (1994) performed such measurements for selected rock samples from the SG-3 bore-hole. A comparison of limited (12 samples, 15 cm total length) high-pressure velocity measurements with sonic log and VSP data showed some agreement (Vernik et al., 1994). Based on this comparison, Vernik et al. (1994) explain all depth intervals with relatively low velocities by the combined effects of variations in lithology and rock fabric only. All other possibilities, as free-water-filled in situ microcracks (e.g. Kremenetsky, 1990) or tectonically induced dilatancy (e.g. Mints et al., 1987) are neglected. The presence of subhorizontal seismic reflections in the Kola area at a depth of 7.5–8.5 km found on wide angle reflection and deep seismic sounding data (e.g. Mints et al., 1987; Pavlenkova, 1991) is explained by Vernik et al. (1994) by the variations in amphibolite bodies' concentration.

Another approach to correlate lithologies with seismic velocities was introduced by Babeyko et al. (1994). They have used a petrophysical modeling technique to calculate intrinsic (crack-free) elastic properties in the lower part of the Kola borehole (6.84–10.53 km) from bulk chemical compositions of core samples. Calculations were performed for a total of 896 core samples. Babeyko et al. (1994) used the comprehensive method of velocity modeling. First they compiled the detailed lithologic cross-section of the Archean part of the Kola bore-

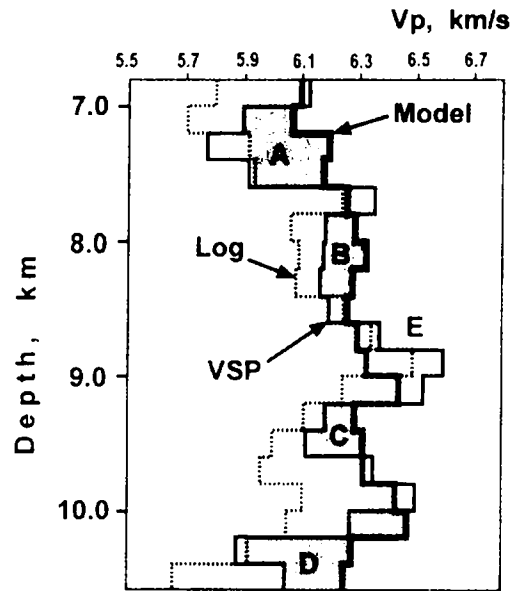


Fig. 7. Zones in the Archean section of the SG-3 (shaded areas) where measured velocities are lower than the intrinsic (crack-free) ones. Comparison is based on the results of petrophysical modeling (Babeyko et al., 1994) with the interval P-wave velocities from the observed VSP and acoustic log data. All velocity values are averaged at 200-m intervals.

hole including 554 individual layers, and only after that, they estimated crack-free isotropic properties of all the layers using calculations for core samples and lithologic information. The results of such calculations averaged at 200-m intervals are presented in Fig. 7 in comparison with velocities obtained from the acoustic log and the deepest Russian VSP (least-squares inversion of travel times performed in the present study).

The shaded areas A, B, C, and D on the velocity plot in Fig. 7 correspond to the depth intervals where both sonic and VSP velocities are lesser than the intrinsic isotropic 'crack-free' velocities. Especially large velocity contrasts are observed for zones A (7.0 km deep) and D (10.0 km): 0.3 and 0.4 km/s, respectively. Zone A corresponds to the fault zone just below Pr–Ar contact and correlates with a group of reflections R5 (Fig. 2) dipping in the same general direction as the layers of the whole Pechenga complex. All other coherent events below the group of reflections R5 are subhorizontal with reflection R8 being the strongest and most laterally continuous (more than 5 km). The reflections R6

and R7 (Fig. 2) correspond to the velocity contrasts between zones B–E and E–C (Fig. 7), respectively. As reported by Lanev et al. (1987), amphibolites are mainly in conformable occurrence with gneisses and contacts form an angle of about 40–60° with the borehole axis. Gneisses of the upper parts of the Archean complex (down to a depth of 9.45 km in the borehole section) are widely developed at the surface north from the SG-3. These facts force us to look for another explanation of the origin of subhorizontal reflections R6–R8, rather than excess of amphibolite bodies.

The effect of fluid-filled voids and anisotropy due to preferred minerals orientation (PMO) can be a reasonable explanation in the case of subhorizontal reflections. The Archean biotite–plagioclase gneisses in the borehole are foliated, and the foliation plane has an inclination of 40–60° to the borehole axis (Kozlovsky, 1987). Taking this into account, Babeyko et al. (1994) performed calculations of velocity deviations from isotropic values in Kola gneisses with average biotite content. They found that anisotropy due to PMO should not lower P-wave velocities more than 5%. Comparison of isotropic crack-free velocity calculations with VSP P-wave velocities shows that anisotropy due to PMO is not enough to account for a velocity reduction (7–8%) in zones A and D (Fig. 7). That is why, we propose fluid-filled voids as major mechanism generating subhorizontal reflections.

The structure of fractures and pore space of the Kola core samples have been studied by many authors (e.g. Kozlovsky, 1987; Morrow et al., 1994; Abdrakhimov et al., 1996). All the investigators agree that many of the observed microcracks resulted from drilling-induced damage, but some of the fractures have characteristics clearly suggesting that they have formed naturally (e.g. Morrow et al., 1994, fig. 5; Abdrakhimov et al., 1996). To clarify the nature of fluid and its effect on rocks, Abdrakhimov et al. (1996) performed special experiments in a 'thermal pressure chamber', which allowed variation of temperature up to 300°C, hydrostatic pressure up to 200 MPa, and deviatoric uniaxial compression up to sample destruction. The experiments were carried out with samples (gneisses and amphibolites) taken from the surface near the SG-3 wellhead. It was established (Abdrakhimov et al., 1996) that subcritical

opening of intergranular space in a crystalline rock becomes possible only with the presence of water. Neither pressure, nor temperature alone do not cause subcritical rock damage. The occurrence of subcritical crustal rock destruction due to stress corrosion has already been documented (e.g. Kerrich et al., 1981; Etheridge, 1983). The particular importance of the work by Abdrakhimov et al. (1996) is that they have estimated the 9–12 km depth interval in the Kola SG-3 section to be the most favorable for stress corrosion cracking. At greater depth, with temperatures increasing to 200°C, this process is changed by crystallization and crack healing. The CDP seismic section incorporates the most prominent subhorizontal reflection R8 at a depth of 10 km (Fig. 2). Approximately the same depth generates subhorizontal reflections recorded on 1992 Kola VSPs (Figs. 4 and 5, reflections C). The maximum helium concentration at a depth of 10 km and increased water inflow (Kozlovsky, 1987) together make the rock-destruction process at 9–12 km, caused by stress corrosion, the most probable explanation of the observed subhorizontal reflectivity. The subhorizontal character of seismic reflectivity also finds its explanation in stress corrosion effect, because of approximately linear P–T distribution in the upper crust.

6. Summary

The Kola CDP section is highly reflective; dipping reflections are generated from lithologic contacts within the supracrustal series and from shear zones. Reflectivity of several zones including a major shear zone at 4.5 km is enhanced by fluid-filled fractures indicated by VSP interval velocities that are too low for non-porous crystalline rocks. Shear zone reflectivity is also enhanced by anisotropy. Reflections may be caused by compositional boundaries, shear zones, anisotropy and fluid-filled voids or some combination thereof. Horizontal reflections are most common in the Archean below 6.8 km, but are also found crossing dipping reflections throughout the CDP profile. No horizontal dips or layers are observed in the core material so no evidence exists for the presence of horizontal dikes to explain the reflections as has been suggested earlier. Interval velocities determined from VSPs are lower than intrinsic rock velocities in the Archean section and

also for the LFZ. The lowered seismic velocity is attributed to fluid-filled microcracks and the horizontal reflections to fluid-filled fractures. Results suggest the presence of fluids down to a depth of at least 12 km in the upper crust; the presence of these fluids lowering seismic velocity causes estimates of upper crustal composition to be too felsic. This may be a widespread phenomenon which means that global estimates of crustal composition based on seismic velocity are biased toward compositions that are too felsic.

Acknowledgements

Thanks are due to both National Science Foundation (Grant EAR-9118600) and RossComNedra for financial support. The authors would like to thank D. Guberman for access to the Kola Superdeep Borehole, Dr. Yu. Kuznetsov for providing us with original log information, and Dr. M. Lizinsky for providing access to the additional Russian deep VSP data. We also wish to thank C. Humphreys and the other members of international seismic team who made the acquisition possible under difficult field conditions. We thank C. Juhlin, H. Harjes, S. Klemperer, and W. Mooney, for many helpful comments and suggestions.

References

- Abdrakhimov, M.Z., Kuznetsov, Yu.I., Zonn, M.S., 1996. Pore space structure of deep crustal rocks from the Kola Overdeep drilling data. *Phys. Solid Earth* 32 (5), 426–436. Translated from *Fizika Zemli* (Russia).
- Babeyko, A.Yu., Sobolev, S.V., Sinelnikov, E.D., Smirnov, Yu.P., Derevchikova, N.A., 1994. The Kola Borehole from bulk chemical composition of core samples. *Surv. Geophys.* 15, 545–573.
- Berthelsen, A., Marker, M., 1986. Tectonics of the Kola collision suture and adjacent Archean and Early Proterozoic terrains in the northeastern region of the Baltik shield. In: Galson, D.A., Mueller, St. (Eds.), *The European Geotraverse, Part 1*. *Tectonophysics* 126, 31–55.
- Carr, B.J., Smithson, S.B., Karaev, N.A., Ronin, A., Garipov, V., Kristofferson, Y., Digranes, P., Smythe, D., Gillen, C., 1996. Vertical seismic profile results from the Kola Superdeep Borehole, Russia. *Tectonophysics* 264, 295–307.
- Christensen, N.I., 1989. Reflectivity and seismic properties of the deep continental crust. *J. Geophys. Res.* 94 (B12), 17793–17804.
- Digranes, P., Kristofferson, Y., Karaev, N., 1996. An analysis of shear waves observed in VSP data from the superdeep well at Kola, Russia. *Geophys. J. Int.* 126, 545–554.
- Etheridge, M.A., 1983. Differential stress magnitudes during regional deformation and metamorphism: upper bound imposed by tensile fracturing. *Geology* 11, 231–234.
- Fountain, D.M., Hurich, C.A., Smithson, S.B., 1984. Seismic reflectivity of mylonite zones in the crust. *Geology* 12, 195–198.
- Fuchs, K., 1969. On the properties of deep crustal reflections. *J. Geophys.* 35, 133–149.
- Gibson, R.L., Ben-Menahem, A., 1991. Elastic wave scattering by anisotropic obstacles: application to fractured volumes. *J. Geophys. Res.* 96, 19905–19924.
- Hohrath, A., Bram, K., Hamitzsch, C., Hubral, P., Kästner, U., Lüschen, E., Rühl, T., Schruth, P.K., Söllner, W., 1992. Evaluation and interpretation of VSP-measurements in the KTB-Oberpfalz pilot borehole. *Sci. Drill.* 3, 89–99.
- Juhlin, C., 1990. Interpretation of reflectors in the Siljan Ring area based on results from the Gravberg-1 borehole. *Tectonophysics* 173, 345–360.
- Karus, E.W., Kuznetsov, O.L., Kuznetsov, Y.I., Rudenko, G.E., Lizinsky, M.D., Litvinenko, I.V., Kudzimsky, L.I., 1987. Seismic investigations in the Borehole. In: Kozlovsky, Y.A. (Ed.), *The Superdeep Well of the Kola Peninsula*. Springer-Verlag, Berlin, pp. 351–358.
- Kerrick, R., La Tour, T.E., Barnet, R.L., 1981. Mineral reactions participating in intragranular fracture propagation: implications for stress corrosion cracking. *J. Struct. Geol.* 3, 77–87.
- Kozlovsky, Ye.A. (Ed.), 1987. *The Superdeep Well of the Kola Peninsula*. Springer-Verlag, Berlin, 558 pp.
- Kremenetsky, A.A., 1990. The geological nature of seismic boundaries in the continental crust. In: Fuchs, K., Kozlovsky, Ye.A., Krivtsov, A.I., Zoback, M.D. (Eds.), *Super-Deep continental drilling and deep geophysical sounding*. Springer-Verlag, Berlin, pp. 353–363.
- Lanew, V.S., Nalivkina, E.B., Vakhrusheva, V.V., Golenkina, E.A., Rusanov, M.S., Smirnov, Y.P., Suslova, S.N., Duk, G.G., Koltsova, T.V., Maslennikov, V.A., Timofeev, B.V., Zaslavsky, V.G., 1987. Geological section of the well. In: Kozlovsky, Y.A. (Ed.), *The Superdeep Well of the Kola Peninsula*. Springer-Verlag, Berlin, pp. 40–73.
- Levander, A., Hobbs, R.W., Smith, S.K., England, R.W., Synder, D.B., Holliger, K., 1994. The crust as a heterogeneous 'optical' medium, or 'crocodiles in the mist'. *Tectonophysics* 232, 281–297.
- Melezhik, V.A., Sturt, B.A., 1994. General geology and evolutionary history of the early Proterozoic Polmak-Pasvik-Pechenga-Imandra/Varzuga-Ust'Ponoy Greenstone Belt in the northeastern Baltic Shield. *Earth-Sci. Rev.* 36, 205–245.
- Mints, M.V., Kolpakov, N.I., Lanew, V.S., Rusanov, M.S., 1987. The character of the subhorizontal seismic boundaries within the upper part of the Earth's crust (according to data from the Kola Ultradeep Well). *Geotectonics* 21 (5), 444–451.
- Mooney, W.D., Meissner, R., 1992. Multi-genetic origin of crustal reflectivity: a review of seismic reflection profiling of the continental crust and Moho. In: Fountain, D.M., Arculus, R., Kay, R.W. (Eds.), *Continental Lower Crust - Develop-*

- ments in *Geotectonics*, Vol. 23, Elsevier, Amsterdam, pp. 45–80.
- Morrow, C., Lockner, D., Hickman, S., Rusanov, M., Röckel, T., 1994. Effects of lithology and depth on the permeability of core samples from the Kola and KTB drill holes. *J. Geophys. Res.* 99, 7263–7274.
- Pavlenkova, N.I., 1991. The Kola superdeep drillhole and the nature of seismic boundaries. *Terra Nova* 4, 117–123.
- Rector, J.W., 1988. Acquisition and Preliminary analysis of oriented multicomponent multi-offset VSP data: DOSECC Cajon Pass Deep Scientific Drillhole. *Geophys. Res. Lett.* 15, 1061–1064.
- Rudnick, R.L., Fountain, D.M., 1995. Nature and composition of the continental crust: a lower crustal perspective. *Rev. Geophys.* 33 (3), 267–307.
- Smithson, S.B., Shive, P.N., Brown, S.K., 1977. Seismic reflections from Precambrian crust. *Earth Planet. Sci. Lett.* 37, 333–338.
- Stewart, R.R., 1984. VSP interval velocities from traveltimes inversion. *Geophys. Prospect.* 32, 608–628.
- Valasek, P.A., Snoke, A.W., Hurich, C.A., Smithson, S.B., 1989. Nature and origin of seismic reflection fabric, Ruby-East Humboldt metamorphic core complex, Nevada. *Tectonics* 8, 391–415.
- Vernik, L., Hickman, S., Lockner, D., Rusanov, M., 1994. Ultrasonic velocities in cores from the Kola Superdeep well and the nature of subhorizontal seismic reflections. *J. Geophys. Res.* 99, 24209–24219.